

ARTICLE OPEN



Exploring the role of neuronal-enriched extracellular vesicle miR-93 and interoception in major depressive disorder

Kaiping Burrows^{1,11}✉, Leandra K. Figueroa-Hall^{1,2,11}, Jennifer L. Stewart^{1,2}, Ahlam M. Alarbi³, Rayus Kuplicki¹, Bethany N. Hannafon⁴, Chibing Tan³, Victoria B. Risbrough^{5,6}, Brett A. McKinney⁷, Rajagopal Ramesh⁸, Teresa A. Victor¹, Robin Aupperle^{1,2}, Jonathan Savitz^{1,2}, T. Kent Teague^{1,2,3,9,10}, Sahib S. Khalsa^{1,2} and Martin P. Paulus^{1,2}

© The Author(s) 2024

Major depressive disorder (MDD) is associated with interoceptive processing dysfunctions, but the molecular mechanisms underlying this dysfunction are poorly understood. This study combined brain neuronal-enriched extracellular vesicle (NEEV) technology and serum markers of inflammation and metabolism with Functional Magnetic Resonance Imaging (fMRI) to identify the contribution of gene regulatory pathways, in particular micro-RNA (miR) 93, to interoceptive dysfunction in MDD. Individuals with MDD ($n = 41$) and healthy comparisons (HC; $n = 35$) provided blood samples and completed an interoceptive attention task during fMRI. EVs were separated from plasma using a precipitation method. NEEVs were enriched by magnetic streptavidin bead immunocapture utilizing a neural adhesion marker (L1CAM/CD171) biotinylated antibody. The origin of NEEVs was validated with two other neuronal markers - neuronal cell adhesion molecule (NCAM) and ATPase Na⁺/K⁺ transporting subunit alpha 3 (ATP1A3). NEEV specificities were confirmed by flow cytometry, western blot, particle size analyzer, and transmission electron microscopy. NEEV small RNAs were purified and sequenced. Results showed that: (1) MDD exhibited lower NEEV miR-93 expression than HC; (2) within MDD but not HC, those individuals with the lowest NEEV miR-93 expression had the highest serum concentrations of interleukin (IL)-1 receptor antagonist, IL-6, tumor necrosis factor, and leptin; and (3) within HC but not MDD, those participants with the highest miR-93 expression showed the strongest bilateral dorsal mid-insula activation during interoceptive versus exteroceptive attention. Since miR-93 is regulated by stress and affects epigenetic modulation by chromatin re-organization, these results suggest that healthy individuals but not MDD participants show an adaptive epigenetic regulation of insular function during interoceptive processing. Future investigations will need to delineate how specific internal and external environmental conditions contribute to miR-93 expression in MDD and what molecular mechanisms alter brain responsivity to body-relevant signals.

Translational Psychiatry (2024)14:199; <https://doi.org/10.1038/s41398-024-02907-x>

INTRODUCTION

Interoception refers to the nervous system's ability to sense, interpret, and integrate internal bodily signals across conscious and unconscious levels [1]. Individuals with major depressive disorder (MDD) often report dysregulated interoceptive awareness, or abnormal experiences of their internal body states [2–5]. It has been argued that, within the context of depression, the brain is rigidly insensitive to interoceptive signals and as a result fails to efficiently predict and regulate the body's metabolic needs [6]. The insular cortex likely integrates interoceptive signals with emotionally salient information during conscious as well as unconscious comparisons of anticipated versus experienced bodily states, a process which relies on the management of interoceptive prediction and prediction-error signals, embodied emotional signals, and self-related signals [7–9]. Moreover, a

recent functional magnetic resonance imaging (fMRI) meta-analysis identified blunted activity of the left dorsal mid-insula in patients with MDD relative to healthy individuals across interoceptive awareness paradigms, suggesting that disrupted mid-insular activation may represent a neural marker and a putative target for novel interventions in depression [10].

Although the cellular and molecular processes resulting in altered interoception in MDD are only beginning to be understood [11], several hypotheses have been advanced. Among them is the notion that elevated levels of pro-inflammatory cytokines in some depressed individuals result in a decoupling of afferent interoceptive input from interoceptive predictions, leading to increased prediction-error signals [12, 13]. Dysregulation of both the innate and adaptive immune systems is consistently described in depressed patients [14] and increased peripheral inflammatory

¹Laureate Institute for Brain Research, Tulsa, OK, USA. ²Oxley College of Health and Natural Sciences, University of Tulsa, Tulsa, OK, USA. ³Departments of Surgery and Psychiatry, School of Community Medicine, The University of Oklahoma, Tulsa, OK, USA. ⁴Department of Obstetrics and Gynecology, University of Oklahoma Health Sciences Center, Oklahoma City, OK, USA. ⁵Center of Excellence for Stress and Mental Health, La Jolla, CA, USA. ⁶Department of Psychiatry, University of California, San Diego, La Jolla, CA, USA. ⁷Department of Mathematics and Computer Science, University of Tulsa, Tulsa, OK, USA. ⁸Department of Pathology, University of Oklahoma Health Sciences Center, Oklahoma City, OK, USA. ⁹Department of Biochemistry and Microbiology, The Oklahoma State University Center for Health Sciences, Tulsa, OK, USA. ¹⁰Department of Pharmaceutical Sciences, The University of Oklahoma College of Pharmacy, Oklahoma City, OK, USA. ¹¹These authors contributed equally: Kaiping Burrows, Leandra K. Figueroa-Hall.

✉email: kburrows@laureateinstitute.org

Received: 21 April 2023 Revised: 2 April 2024 Accepted: 10 April 2024

Published online: 27 April 2024

markers have been linked to disturbed brain function in regions including the insula [15]. In addition to immuno-inflammatory activation, neuroendocrine regulators of energy metabolism such as leptin and insulin are involved in homeostatic adjustments and brain circuits integrating homeostatic and mood regulatory responses [16]. Leptin, a peptide hormone with pro-inflammatory properties that functions to maintain energy homeostasis [17], can interact with neural circuitry to increase the likelihood of developing MDD [18]. These findings suggest that mechanistic alterations of interoception in MDD may be related to elevated pro-inflammatory cytokine levels, immune system dysregulation, and disturbances in insula activity, as well as involvement of neuroendocrine regulators of energy metabolism and mood regulation.

Measuring neuronal-enriched extracellular vesicles (NEEVs) enables one to non-invasively examine specific molecular processes in the brain. These molecular findings can be integrated with systems-level signals such as fMRI to gain a better understanding of the biological dysfunction related to specific cognitive or affective processes. Extracellular vesicles (EVs), including exosomes (biogenesis occurring through multivesicular bodies inside the cell; size range ~40 nm to 160 nm) and ectosomes (vesicles that pinch off the surface of the plasma membrane by outward budding; size range ~50 nm to 1 µm in diameter) are released by many cell types and can be associated with immune responses, among others [19]. EVs contain proteins, metabolites, and nucleic acids that can be delivered into recipient cells for intercellular communication, thereby effectively altering their biological responses related to regulation of central and peripheral immunity, and/or metabolic reprogramming [19]. Moreover, NEEVs cross the blood-brain barrier from both directions and are involved in central nervous system (CNS) regulation by micro ribonucleic acid (RNA) (MiR) transmission. MiRs are a class of small non-coding RNAs functioning as key post-transcriptional regulators of gene expression through the destabilization of messenger RNA (mRNA); MiRs are enriched in the CNS and more distinct MiRs are expressed in the brain than in any other tissue [20]. Neuronal MiRs account for 70% of all MiRs in our body that are involved in regulating neurogenesis and neuroplasticity [21]. It is important to note that MiRs carried from the brain may enter into blood circulation during major depressive episodes [22]. Identifying MiRs related to neuronal development, inflammation, and metabolic pathways can elucidate body-brain connections and how they differ as a function of MDD presence versus absence.

One such MiR, microRNA-93-5p (miR-93), is a member of the miR-106b-25 cluster, located on chromosome 5 [23], and has been implicated in the regulation of neural progenitor cell proliferation and neuronal differentiation [24]. miR-93 can regulate neurogenesis and neuronal growth [25] and target mRNAs involved in metabolic signaling [26]. miR-93 reduces inflammatory cytokine expression, including interleukin (IL)-1 beta (IL-1β), tumor necrosis factor (TNF), and IL-6 through signal transduction/activation of the transcription 3 (STAT3) signaling pathway [27, 28]. Another pathway regulated by miR-93, the toll-like receptor 4 (TLR4) inflammatory pathway, has been postulated as one of the key players implicated in the increased inflammatory response in depressed individuals [29]. For instance, research indicates that miR-93 regulates the TLR4/NF-κB pathway [30, 31] and EV-derived miR-93 protects lipopolysaccharide (LPS)-induced cell injury by inhibiting TNF activation [32]. There is also some evidence showing the link between dysregulated miR-93 and other processes perturbed in depression such as insulin resistance [33, 34], adipogenesis [35], which could make it a therapeutic target for obesity and the metabolic syndrome [36, 37], and chromatin remodeling [38, 39].

Given the roles of miR-93 in regulating neuronal axogenesis, inflammation, and metabolism, the current study aimed to link these molecular processes to previously described mid-insula dysfunction during interoceptive processing in depression by

integrating brain fMRI and NEEV technology. A sub-sample of MDD and healthy comparison (HC) participants from the Tulsa 1000 (T1000) project [40] completed an interoceptive awareness task during fMRI and provided blood for isolation and enrichment of NEEVs and immunoassays. We evaluated the role of miR-93 to investigate whether MDD patients differed from HC in: (1) NEEV miR-93 expression; (2) the relationship between NEEV miR-93 expression and inflammatory and metabolic markers; and (3) the relationship between NEEV miR-93 expression and brain activity during interoceptive versus exteroceptive attention.

MATERIALS AND METHODS

Participants

Participants in this study were drawn from the first 500 individuals who completed baseline assessments as part of the T1000 project, a naturalistic longitudinal study of 1000 individuals including healthy and treatment-seeking individuals with mood, anxiety, substance use and eating disorders [40]. The T1000 study was conducted at the Laureate Institute for Brain Research (LIBR) in Tulsa, Oklahoma, United States. Baseline assessments occurred between 1/01/2015 and 12/21/2017. The T1000 project was approved by the Western Institutional Review Board and performed in accordance with the Declaration of Helsinki (ClinicalTrials.gov identifier: NCT02450240, "Latent Structure of Multi-level Assessments and Predictors of Outcomes in Psychiatric Disorders"). Participants provided written informed consent and received compensation for their participation.

Participants were recruited from the Laureate Psychiatric Clinic and Hospital, other local mental health providers, and the general community through radio, online, newspaper, and other media advertisements in Tulsa and the surrounding regions of Oklahoma. Participants were evaluated for Diagnostic and Statistical Manual of Mental Disorders (DSM)-IV or DSM-5 diagnoses determined by the Mini International Neuropsychiatric Inventory (MINI) [41]. All participants in the MDD groups entered the T1000 study with significant depressive symptoms (the Patient Health Questionnaire (PHQ-9) ≥ 10 [42]) and met DSM criteria for a past and/or current MDD diagnosis. See Victor et al and colleagues for complete sample size, demographic and screening measures [40].

To determine whether individuals with depression show evidence for altered cellular processing related to interoception, only MDD and HC subjects were included in the present analysis. Our previous study using participants from this sample suggested that there was no statistically significant evidence for blood oxygen level-dependent (BOLD) signal differences between un-medicated MDD and MDD with use of selective serotonin reuptake inhibitors (SSRI) on the visceral interoceptive awareness (VIA) task [43]; therefore, both unmedicated and SSRI-medicated subjects were included in this analysis. MDD subjects taking selective norepinephrine reuptake inhibitors (SNRI), or taking various other antidepressants were excluded from the current analysis. Participants were also excluded if they had inflammation or metabolic related disease (e.g., autoimmune disease, inflammatory bowel disease, or diabetes), or were taking anti-inflammatory or anti-diabetic drugs. In addition, subjects were excluded if they had poor quality or missing VIA fMRI data. Finally, 41 MDD and 35 HC participants remained for data analysis (see Table 1).

The following demographic and clinical ratings were assessed: (1) age, sex, education, employment status, International Physical Activity Questionnaire (IPAQ), and body mass index (BMI) metrics; and (2) the Patient-Reported Outcomes Measurement Information System (PROMIS) [44] depression scale.

Neuronal-enriched EV

See Supplemental Methods. EV Track ID#EV210507.

Blood collection. Venous blood was collected during the baseline assessment in BD Vacutainer EDTA Blood Collection tubes, which were then transported to the University of Oklahoma Integrative Immunology Center (IIC) within two hours of collection. Blood tubes were centrifuged at 1300 × g for 10 min (min) at room temperature (RT); plasma was removed, aliquoted, and then stored at -80 °C until analysis.

EV separation. The EV separation method was adapted from our previous publication [45]. Plasma was thawed on ice, then centrifuged at 3000 × revolutions per minute (rpm) for 15 min. 3.5 microliters (µL) of Purified Thrombin (500 U/mL) (System Biosciences, CA, United States; Catalog #

Table 1. Sample demographics and clinical characteristics.

Group	MDD (n = 41) Mean (sd)	HC (n = 35) Mean (sd)	p value
Age	34.22 (11.63)	30.03 (9.85)	0.10 ^a
Sex = Male (%)	11 (26.8)	14 (40.0)	0.33 ^b
IPAQ category (%)			0.01 ^b
HEPA Active	10 (20.4)	20 (58.8)	
Minimally Active	11 (26.8)	8 (23.5)	
Inactive	20 (48.8)	6 (17.6)	
IPAQ MET-minutes per week	2412.40 (3470.15)	4791.00 (3872.39)	<0.01 ^a
Body Mass Index	30.41 (4.61)	26.44 (4.95)	<0.01 ^a
PROMIS Depression Score	63.20 (6.55)	42.49 (6.61)	<0.01 ^a

MDD major depressive disorder, HC healthy control, IPAQ International Physical Activity Questionnaire, PROMIS, Patient-Reported Outcomes Measurement Information System Depression Score.

^aTwo sample *t*-test.

^b χ^2 test.

TMEXO-1) were added to 350 μ L of plasma to make a final concentration of 5 U/mL. After incubating plasma/thrombin for 5 min at RT and centrifuging plasma/thrombin at 10,000 rpm at RT for 5 min, 300 μ L of plasma were used for EV separation; the remaining plasma and fibrinogen pellet were discarded. Briefly, 76 μ L of ExoQuick Exosome Precipitation Solution (System Biosciences, CA, USA; Catalog #EXOQ5A-1) were added to 300 μ L of plasma, incubated 30 min on ice, and then centrifuged at 1500 \times *g* at 4 °C for 30 min. After removing supernatants, the pellets were centrifuged at 1500 \times *g* at 4 °C for an additional 5 min to remove all traces of supernatant. EV pellets were re-suspended in 300 μ L of 1 \times phosphate buffered saline (PBS) (Thermo Fisher Scientific, United States; Catalog #AM9625) with 1 \times Halt protease and EDTA-free phosphatase inhibitor cocktail (Thermo Fisher Scientific, United States; Catalog #78425). Finally, 150 μ L of EV were used for immunochemical enrichment, and the remaining EV aliquots were stored at -80 °C for future analysis.

NEEV enrichment. EVs were enriched via a magnetic streptavidin bead immunocapture kit targeting the neural adhesion marker, L1CAM (CD171) biotinylated antibody; for schematic cartoon of the NEEV enrichment (see Burrows et al. [45]). This method for enriching NEEVs in blood samples has been validated [45–48]. The CD171 (L1CAM, neural adhesion protein) marker was used for NEEV enrichment due to its high and relatively specific expression in neurons and low levels of expression in many other cell types [46].

Flow cytometry. Once NEEVs were captured and stabilized, the bead/antibody/EV complex was coupled to the EV marker – CD63 fluorescein isothiocyanate (FITC) and neuronal marker – CD171 Allophycocyanin (APC) fluorescent tags and subsequently analyzed by flow cytometry to confirm EV capture and NEEV enrichment.

Western blot. EVs, NEEVs, EV-depleted plasma, total EV after enrichment, and cells were denatured directly in a 4 \times Laemmli sample loading buffer and separated by SDS-PAGE using Mini PROTEAN[®] TGX[™] precast gels (Bio-Rad, Catalog # 4561044). Separated proteins were transferred onto polyvinylidene difluoride (PVDF) membranes using a Trans-Blot[®] Turbo transfer system (Bio-Rad, Catalog #1704156). Primary antibodies used include CD171 (1:1000, Invitrogen, Catalog #13-1719-82), NCAM/CD56 (1:250, Invitrogen, Catalog # MA5-11563), ATP1A3 (1:500, US Biological, Catalog # 032268-APC), CD81 (1:1000, Santa Cruz, Catalog #SC-166029), Alix (1:1000, Santa Cruz, Catalog #SC-53540), calnexin (1:1000, Cell Signaling, Catalog #2679), and APOA1 (1:500, Santa Cruz, Catalog # SC-376818).

Transmembrane electron microscopy (TEM). For EM, EV samples suspended in water were fixed in 2% paraformaldehyde. Fixed samples were absorbed onto formvar coated copper grids for 20 min. Samples were then fixed in 1% glutaraldehyde for 5 min. After being rinsed in distilled water, samples were stained with 2% uranyl acetate for 1 min. Excess liquid was

wicked off the grid using filter paper, and grids were stored at room temperature until imaging. Imaging was performed on a Hitachi H7600 microscope equipped with an AMT NanoSprint 1200 camera at the Oklahoma Medical Research Foundation (OMRF) imaging core.

Particle size and concentration analysis. The particle concentration and size of EVs and NEEVs were measured using microfluidic resistive pulse sensing (MRPS) method with the Spectradyne nCS1[™] instrument (Spectradyne Particle Analysis, Signal Hill, CA, USA).

miRNA purification. Qiagen miRNeasy Micro Kit (QIAGEN, United States; Catalog #217084) was used for purification of total RNA including miRNA from EVs and NEEVs according to the manufacturer's protocol. Small RNA concentration was measured using an Agilent Small RNA Kit (Agilent, United States; Catalog #5067-1548) on a Bioanalyzer 2100 instrument (Agilent, United States). RNA samples were stored at -80 °C until sequencing.

miRNA sequencing and data processing. RNA samples were sent to the Oklahoma Medical Research Foundation (OMRF) Clinical Genomics Center for Next Generation Sequencing (NGS). Briefly, miRNA libraries were generated with a Qiagen QIAseq MiR library preparation kit and NGS was performed on an Illumina NextSeq HO SR75. Raw sequence FASTQ files received from OMRF were imported to the Partek Flow Software for data analysis. Adapters from 3' end were trimmed from the raw reads after a quality check, with bases trimmed from both ends, and then aligned to the human genome hg38 using Bowtie alignment. Next, the aligned reads were quantified against the human miRbase mature microRNAs version 22 and reads from miR genes were normalized and scaled to reads per million for statistical data analysis.

Immunoassays

Serum interleukin 1 receptor antagonist (IL-1ra) concentrations were measured with the Human IL-1ra/IL-1F3 Quantikine ELISA kits (R & D Systems, Minneapolis, USA). Serum TNF (TNF- α) and IL-6 concentrations were measured with the Proinflammatory Panel 1 Human Kit (Meso Scale Diagnostics, Maryland, USA), and C-reactive protein (CRP) was analyzed with Vascular Injury Panel 1 Human Kit (Meso Scale Diagnostics, Maryland, USA). The Human Leptin, Insulin Kit (Meso Scale Diagnostics, Maryland, USA) was used to analyze serum leptin concentrations. All serum samples were tested in duplicate. The intra- and inter-assay coefficients of variation (CV) were 3.1% and 15.6% (IL-1ra), 4.2% and 7.0% (IL-6), 3.1% and 12.1% (TNF- α), 2.5% and 10.0% (CRP), and 6.6% and 8.9% (leptin), respectively.

Neuroimaging

Each participant completed a structural MRI scan followed by fMRI scanning while performing the VIA task.

MRI acquisition. MRI images were acquired on two identical General Electric Discovery MR750 (GE Healthcare, Milwaukee, WI) whole-body 3-Tesla MRI scanners. The structural scan was acquired using a T1-weighted magnetization-prepared rapid gradient-echo (MPRAGE) sequence. Anatomical imaging parameters were repetition time (TR)/echo time (TE) = 5/2.012 ms, field of view (FOV) = 240, 186 axial slices, 0.9 mm slice thickness, 256 \times 256 matrix, voxel volume = 0.938 \times 0.938 \times 0.9 mm³, flip angle = 8°, acceleration factor R = 2, inversion time = 725 ms. A single-shot gradient-recalled echo-planar imaging (EPI) sequence with Sensitivity Encoding (SENSE) depicting BOLD contrast was used for functional scans. Functional imaging parameters were TR/TE = 2000/27 ms, FOV/slice = 240/2.9 mm, 128 \times 128 acquisition matrix, 39 axial slices, 180 TRs, flip angle = 78°, SENSE acceleration factor R = 2 in anterior-posterior direction, and voxel volume = 1.875 \times 1.875 \times 2.9 mm³.

Interoceptive awareness task. The VIA task was comprised of two eight-minute runs, each containing interoceptive and exteroceptive conditions. During the interoceptive conditions, the words "heart" and "stomach" cued participants to attend to sensations from that part of the body. During the exteroception (i.e., control) condition, participants attended to the word "target" as it alternated between black and varying shades of gray. Trials lasted 10 seconds (s), and half of trials were followed by a 5-s period for participants to rate stimulus intensity (0 = 'no sensation' to 6 = 'extreme sensation'). Each run included 6 trials per condition (intertrial interval range 2.5–12.5 s). The VIA task has been previously shown to be effective at mapping the neural signal associated with interoceptive attention, including in depressed individuals [5, 49–53].

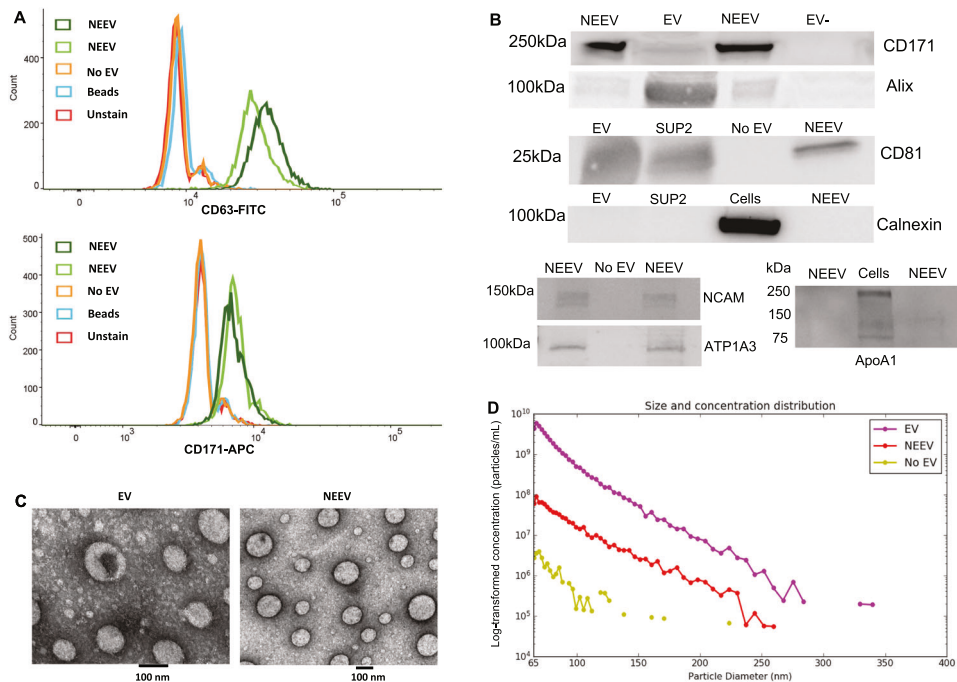


Fig. 1 Characterization of EV and NEEV. **A** Flow cytometry results of neuronal-enriched extracellular vesicles (NEEVs), negative control (No EV), beads and unstained samples with the extracellular vesicle (EV) marker CD63-FITC and NEEV marker CD171-APC. NEEVs were positive for EV marker CD63-FITC and NEEV marker CD171-APC compared to EV-negative control, beads, or unstained samples, as expected. **B** Western blot analysis of NEEV, EV, and EV negative or positive control with NEEV surface marker CD171, EV surface marker CD81, EV internal marker Alix, EV negative marker Calnexin, additional two neuronal markers – neuronal cell adhesion molecule (NCAM) and ATP1A3, and APOA1 as EV contaminant. Note, EV-: EV-depleted plasma; SUP2: total EV after enrichment; No EV: PBS instead of total EV were used for enrichment. Western blot analysis showed that (1) CD171 marker was enriched in NEEVs; (2) EV surface marker CD81 and EV internal marker Alix were present in EVs and NEEVs; (3) EV negative marker Calnexin was not observed in EV or NEEV samples; (4) other two neuronal markers – NCAM and ATP1A3 were present in NEEVs; and (5) EV contaminant marker APOA1 was not observed in NEEV samples. **C** Images of EVs and NEEVs with transmission electron microscopy (TEM); images denote a scale bar of 100 nm. **D** depicts size and concentration analysis of EV, NEEV, and EV-depleted plasma (No EV) using multifluidic resistive pulse sensing (MRPS) with the Spectradyne nCS1TM instrument. MRPS indicates that the majority of EVs and captured NEEVs were in the small EV size range. The average concentration of NEEVs was approximately 1.98×10^{10} particles per mL, which was approximately 30-fold higher than EV-depleted plasma (6.7×10^8 particles per mL). The approximate concentration of EV used for NEEV enrichment was 9.45×10^{10} particles per mL. Note: Y-axis is log-transformed concentration (particles/mL).

fMRI data preprocessing. Single-subject image pre-processing was performed using Analysis of Functional NeuroImages (AFNI) software (<http://afni.nimh.nih.gov/afni>) [54]. The anatomical scan was registered to the first volume of the EPI time-course and then aligned to Montreal Neurological Institute (MNI) space via affine transformation, saving the transformation parameters for application to the EPI data. The first three TRs were discarded from each EPI time-course to allow the fMRI signal to reach steady state, followed by despiking; slice-timing correction and co-registration to anatomical volumes. Motion correction and spatial transformation to MNI space of the EPI data were implemented in a single transformation. The EPI data were then smoothed with a 4 mm Gaussian full-width at half-max smoothing kernel, and signal intensity normalized to reflect percent signal change from each voxel's mean intensity across the time-course. All images were resampled to $2 \times 2 \times 2$ mm³ isometric voxels.

Subject-level fMRI imaging analysis. Each subject's functional imaging data were analyzed using a voxelwise general linear model analysis. Block regressors were convolved with a canonical hemodynamic response function and used to model BOLD responses for heart, stomach, and target conditions. Six motion parameters (three translations and three rotations) were included as nuisance regressors. Censoring was done at the regression step by removing volumes with either a Euclidean norm of the derivatives of the six motion parameters greater than 0.3 mm or greater than 10% outlier voxels, determined by 3dToutcount. Percent signal change during each condition was defined as the estimated beta coefficient from single-subject analysis.

Statistical analysis

Demographic characteristics and clinical ratings. Independent sample *t*-tests examined differences between MDD and HC on age, sex, IPAQ

exercise MET-minutes per week, BMI, and PROMIS depression. A chi square test was used to access sex differences between groups.

NEEV miRNA analysis. Statistical analyses on NEEV miR-93 were conducted in R (version 4.2.0). Scaled miR-93 data (counts per million) were log-transformed due to their non-Gaussian distributions determined by Shapiro-Wilks tests. Outliers were defined as $z = \pm 3$ across subjects and set as missing. Independent sample *t*-tests were used to assess differences between MDD and HC, as well as between un-medicated and SSRI-medicated MDD subjects. In addition, miR-9, a neuronal cell-specific marker [55], was compared between NEEV and EV.

Relationship between NEEV miR-93 expression and inflammatory/metabolic markers. All inflammatory/metabolic markers (IL-1ra, TNF, IL-6, CRP, and leptin) were log-transformed due to their non-Gaussian distributions determined by Shapiro-Wilks tests. Outliers were defined as $z = \pm 3$ across subjects and set as missing. Independent *t*-tests were used to test group differences on IL-1ra, IL-6, and TNF; relationships between NEEV miR-93 expression and IL-1ra, IL-6, and TNF within each group were tested by Pearson's correlations.

Even after log-transformation, the distributions for CRP and leptin were found to be non-Gaussian; therefore, Spearman's correlations were used to test their relationships to NEEV miR-93 expression within each group, and group differences on these two markers were tested using Mann-Whitney-Wilcoxon non-parametric tests. ANOVA tests were used to evaluate slope differences between MDD and HC groups.

Group-level fMRI imaging analysis. AFNI's 3dttest++ was used to assess the whole brain voxel-wise group by NEEV miR-93 interaction on BOLD activation of the interoception versus exteroception contrast. The group statistical map was corrected for multiple comparisons according to our previous

neuroimaging approaches with this task (see Supplemental Methods). BOLD activation of the interoception versus exteroception contrast within clusters with significant group*miR-93 effects were extracted for follow-up analyses. Robust regression tested the slope of different relationships between NEEV miR-93 and BOLD for each significant cluster. False Discovery Rate correction for multiple comparisons was used across the resulting tests.

RESULTS

Demographics and clinical characteristics

The groups did not differ on age, sex, education, or employment status (Table 1). The MDD group reported lower IPAQ physical activity as well as higher BMI and PROMIS depression scores than the HC group.

Characterization of EV and NEEV

Figure 1 shows the results for EV and NEEV characterization following MISEV2018 guidelines [56]. Flow cytometry results (Fig. 1A) showed that NEEVs were positive for EV marker CD63-FITC and NEEV marker CD171-APC compared to EV-negative control, beads, or unstained samples. Western blot analysis (Fig. 1B) showed that: (1) the CD171 marker was enriched in NEEVs; (2) the EV surface marker CD81 and EV internal marker Alix were present in EVs and NEEVs; (3) the EV negative marker Calnexin was not observed in EV or NEEV samples; (4) the two other neuronal markers – neuronal cell adhesion molecule (NCAM) and ATPase Na⁺/K⁺ transporting subunit alpha 3 (ATP1A3) were present in NEEVs; and (5) the EV contaminant marker APOA1 was not observed in NEEV samples. See Supplementary Figs. S1–S7 for images of full-length gels. Additionally, the neuronal cell-specific marker, miR-9, was expressed at a 15-fold higher level in NEEV than EV (Supplemental Fig. S8).

Transmission electron microscopy images of EVs and NEEVs (Fig. 1C) showed that the majority of EVs and captured NEEVs were in the small EV size range (Fig. 1D). The average concentration of NEEVs was approximately 1.98×10^{10} particles per mL, which was approximately 30-fold higher than EV-depleted plasma (6.7×10^8 particles per mL). The approximate concentration of EV used for NEEV enrichment was 9.45×10^{10} particles per mL.

NEEV miRNA results

One outlier from the MDD group was excluded for miR-93 analysis. MDD exhibited significantly lower levels of NEEV miR-93 expression than HC ($p = 0.037$, Cohen's $d = 0.482$) (Fig. 2), a difference that remained after controlling for BMI ($p = 0.035$). In addition, miR-93 expression did not differ between unmedicated and SSRI-medicated MDD individuals ($p = 0.398$).

Immunoassay results

The MDD group exhibited significantly higher levels of IL-1ra ($p = 0.006$, $d = 0.657$), IL-6 ($p = 0.014$, $d = 0.596$), CRP (*wilcoxon* $p < 0.001$, $d = 1.186$), and leptin (*wilcoxon* $p = 0.021$, $d = 0.637$) than HC. Group differences were observed in the slope of the relationship between NEEV miR-93 and serum IL-1ra ($F_{(1, 72)} = 5.71$, $p = 0.020$); serum IL-6 ($F_{(1, 70)} = 5.66$, $p = 0.020$); serum TNF ($F_{(1, 71)} = 4.63$, $p = 0.035$); and serum leptin ($F_{(1, 72)} = 5.27$, $p = 0.025$). Lower NEEV miR-93 expressions were associated with higher serum IL-1ra ($r = -0.39$, $p = 0.013$; Fig. 3A), IL-6 ($r = -0.40$, $p = 0.012$; Fig. 3B), TNF ($r = -0.37$, $p = 0.018$; Fig. 3C), and leptin ($r = -0.34$, $p = 0.035$; Fig. 3D) concentrations in MDD participants but no such relationship was observed in HCs (IL-1ra, $r = 0.11$, $p = 0.528$; IL-6, $r = 0.01$, $p = 0.942$; TNF, $r = 0.13$, $p = 0.457$; leptin $r = 0.00$, $p = 0.996$). No significant correlations were observed between NEEV miR-93 and serum CRP concentrations. Fisher's *r*-to-*z* transformations indicated that the relationship between miR-93 expression and inflammatory/metabolic markers was significantly more negative in MDD than HC for IL-1ra ($z = -2.15$,

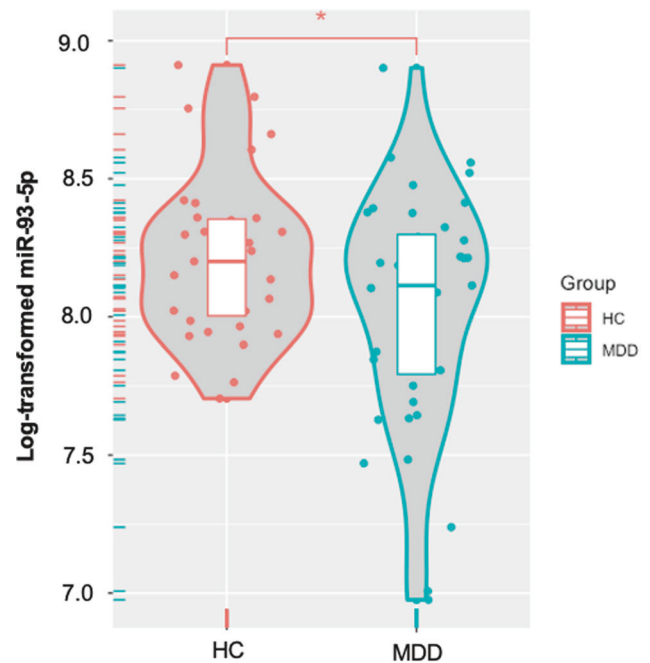


Fig. 2 Differential expression of neuronal-enriched extracellular vesicle (NEEV) microRNA-93-5p (miR-93-5p) between MDD and HC groups. MDD major depressive disorder, HC healthy comparisons. * Indicates that the MDD group exhibited significantly lower levels of NEEV miR-93-5p expression than HC ($p < 0.05$).

$p = 0.016$), IL-6 ($z = -1.80$, $p = 0.036$), and TNF ($z = -2.15$, $p = 0.016$), and trending more negative in MDD than HC for leptin ($z = -1.45$, $p = 0.074$).

Neuroimaging results

There were no significant group activation differences observed outside of the insular cortex, and thus, our analysis focused on clusters of observed insular activation. Specifically, group differences were observed in the slope of the relationship between NEEV miR-93 and the interoception versus exteroception contrast within the left ($F_{(1, 71)} = 6.34$, $p_{\text{corrected}} = 0.014$) and right ($F_{(1, 71)} = 9.75$, $p_{\text{corrected}} = 0.006$) dorsal mid-insula. Within the HC group, higher miR-93 expressions were associated with higher BOLD signal for the interoception versus exteroception contrast within the left ($r = 0.34$, $p_{\text{corrected}} = 0.047$) and right ($r = 0.54$, $p_{\text{corrected}} = 0.002$) dorsal mid-insula, but no such relationship was observed in MDD participants (Fig. 4). Fisher's *r*-to-*z* transformations were applied to this correlation for each group and then compared; the results indicated that the relationship between miR-93 expression and interoception was significantly more positive in HC than MDD for the left ($z = 2.57$, $p = 0.010$) and right ($z = 3.49$, $p < 0.001$) dorsal mid-insula.

DISCUSSION

This study aimed to elucidate the molecular processes underlying previously described mid-insula dysfunction during interoceptive processing in depression using brain NEEV measurement, serum markers of inflammation and metabolism, and whole brain fMRI recording. There were three main findings. Firstly, miR-93 expression in NEEVs was significantly diminished in individuals with MDD compared to HC. Secondly, a unique association emerged in MDD participants, where reduced miR-93 expression in NEEVs correlated with elevated serum concentrations of IL-1ra, IL-6, TNF, and leptin, establishing a connection between miR-93 expression in MDD and heightened inflammation. Lastly, in HC

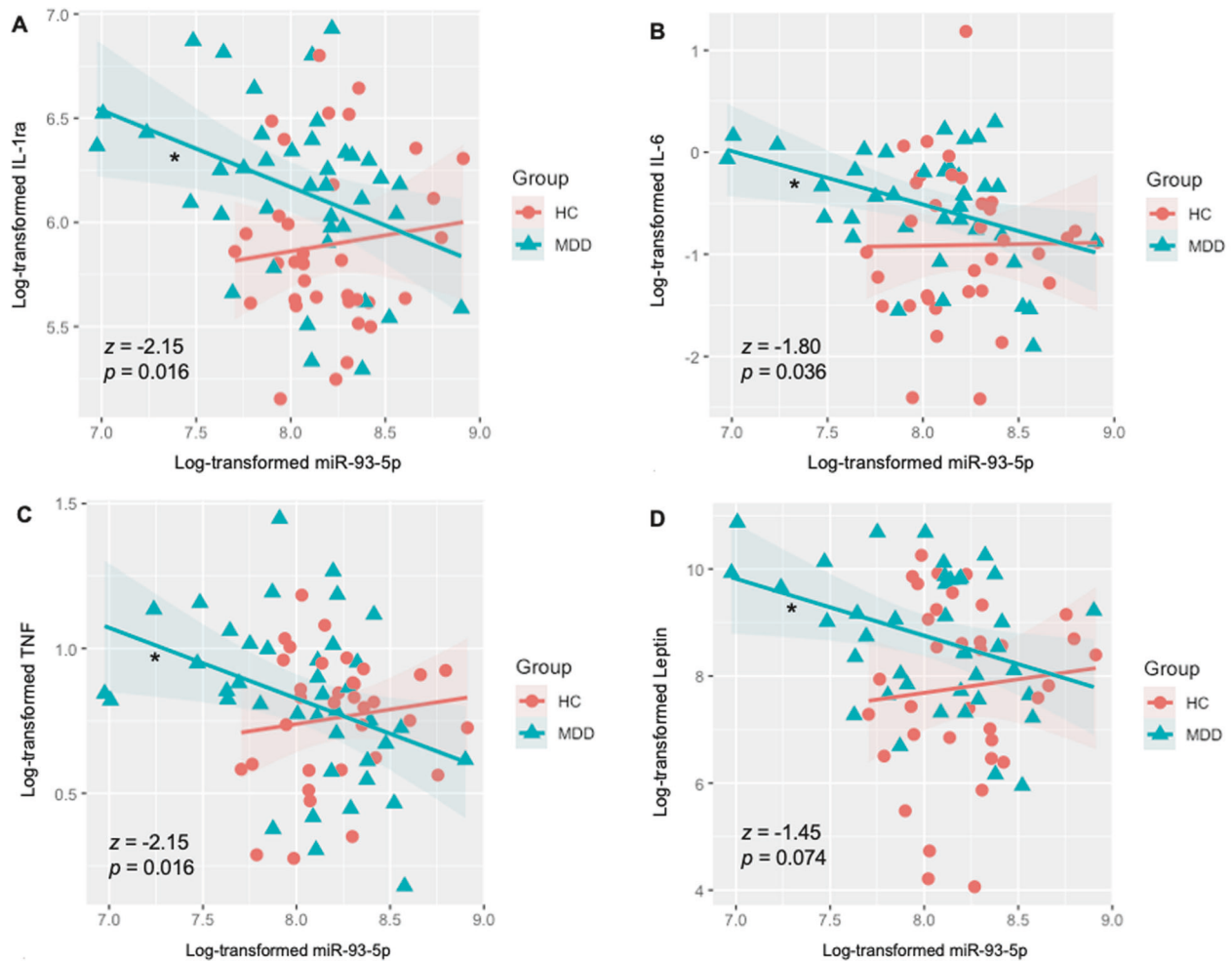


Fig. 3 Differential associations between neuronal-enriched extracellular vesicle miR-93 and serum IL-1ra, IL-6, TNF, and leptin, in the MDD and HC groups. A–D Group differences were observed in the slope of the relationship between NEEV miR-93 and all serum markers. Lower NEEV miR-93 expressions were associated with higher serum **A** IL-1ra, **B** IL-6, **C** TNF, and **D** Leptin concentrations in MDD participants, but no such relationship was observed in HCs. MDD major depressive disorder, HC health comparisons, IL-1ra interleukin-1 receptor antagonist, IL-6 interleukin-6, TNF tumor necrosis factor. z , p , Fisher's r -to- z transformations (MDD>HC). * indicates a significant correlation within the MDD group.

participants, but not in those with MDD, miR-93 expression in NEEVs exhibited a positive correlation with BOLD signals in the left and right dorsal mid-insula during interoception, linking miR-93 regulation to adaptive interoceptive processing in healthy individuals. Taken together, while healthy individuals demonstrate increased responsiveness to stress-induced epigenetic regulation of insular function during interoceptive processing, MDD participants exhibit a failure to do so. This highlights the potential role of insufficient miR-93 signaling and its altered relationship with systems-level interoceptive processing in contributing to interoceptive processing abnormalities in MDD. The pathways unveiled in this study could offer novel therapeutic targets for rectifying interoceptive dysfunction among individuals suffering from depression.

MiR-93 expression was lower in individuals with MDD than those without MDD. To better understand the role of NEEV miR-93 in different neuronal processes, we performed a biological pathway analysis with miRWalk [57] by target mining the full mature miRNA, hsa-miR-93-5p, with miRBaseID. Several genes and biological pathways were identified after filtering with TargetScan, miRDB, and miRTarBase. Several differentially expressed genes were used during Gene Set Enrichment Analysis (GSEA), which identified 210 enriched genes, and 23 (out of 53) biological pathways that were

significant, to include pathways centered on calcium ion transport, memory, and protein ubiquitination (See Supplemental Table S1). The pathways mentioned above are known to play a role in depression; for instance, the lack of ubiquitination of certain proteins [58–60], memory disruption [61, 62], and calcium ion signaling (linked to neuronal excitability and neurotransmitter release) [63, 64], have all been linked to depression. These targets and more may be of interest or offer plausible explanations to the decreased interoceptive signaling found in depressed individuals, given that miR-93 in NEEV is attenuated.

We observed lower NEEV miR-93 associated with higher serum concentrations of inflammatory and metabolic markers, IL-1ra, IL-6, TNF, and leptin within MDD. Extant literature shows that a subset of depressed individuals exhibits increased levels of pro-inflammatory cytokines, as those mentioned here [65–67]. The decreased expression of NEEV miR-93 in MDD, which was not seen in HC, may point to a possible mechanism of elevated inflammation in MDD. This, in part, may be due to the negative regulation of miR-93 on the interleukin receptor associated kinase-4 (IRAK-4), and in turn, suppression of inflammatory cytokines [68, 69], posing a possible target for inflammation-associated depression. Some studies have shown that elevated leptin concentrations and leptin resistance are linked to depression-

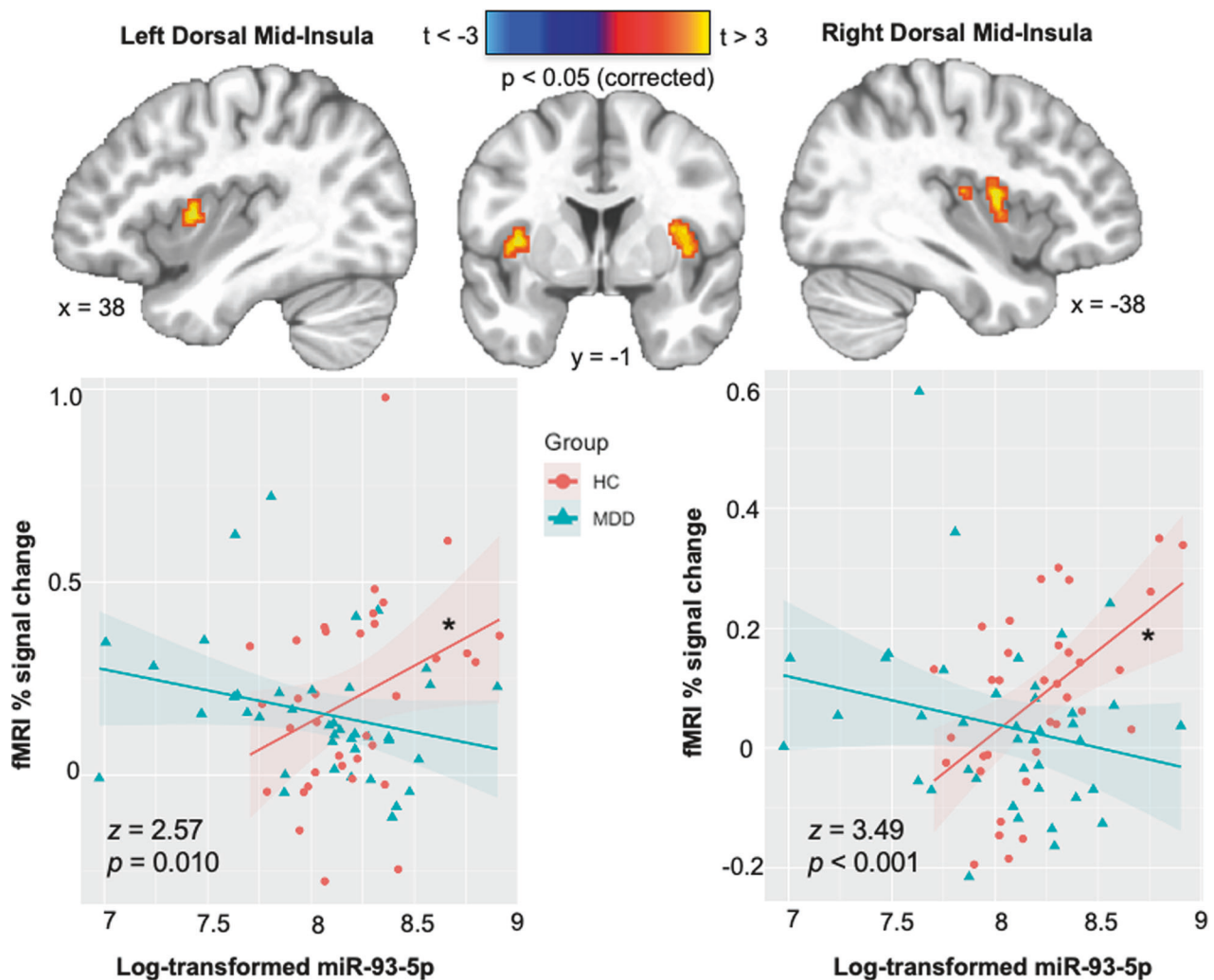


Fig. 4 Differential association between neuronal-enriched extracellular vesicle miR-93 and interoception versus exteroception contrast during the interoceptive awareness task in the MDD and HC groups. MDD major depressive disorder, HC healthy comparisons. Z , p , Fisher's r -to- z transformations (MDD > HC). * Indicates a significant correlation within the HC group ($p < 0.05$).

related appetite increase or atypical features in MDD [13, 70, 71]. In the dataset involved in current analysis, we did observe higher serum leptin concentrations in MDD subjects than HC. The negative association between NEEV miR-93 expression and serum leptin concentration in MDD provides a possible treatment target for MDD with leptin-related metabolic dysfunctions.

We did not observe an association between miR-93 expression and interoceptive signaling in the brains of individuals with MDD, but we did find a relationship between NEEV miR-93 and higher interoception-associated insula activity in healthy individuals. This could suggest a homeostatic role of miR-93 from NEEV during intact interoception, although the precise nature of this relationship is unclear. Consistent with empirical and theoretical findings implicating the role of insular activity in subjective interoceptive and emotional states [72–74], our observation of associations between miR-93 and VIA BOLD signal in left and right dorsal mid-insula might be interpreted to suggest a mechanism whereby the trafficking or regulation of NEEV miR-93 activity is intact and involved in interoceptive processing in healthy individuals, but dysfunctional in depressed individuals. However, this is a speculative notion and warrants further study, particularly with respect to longitudinal assays of the relationship between affective states, NEEV miR-93 activity, and neural indicators of interoception in depression.

Interoception is a process allowing individuals to continuously sense and integrate numerous visceral, physiological signals

including autonomic and nociceptive input, emotional stimuli, hunger signals, and sleep, which are then perceived by the brain during continuous feedback [75]. miR-93-5p regulates many diverse gene products that influence a range of potentially associated processes ranging from inflammation to epigenetic modulation (See Supplementary Fig. S9). It seems plausible that its expression is both a consequence of environmental exposure with long-term consequences, e.g. early life stress [14], or subtle inflammatory processes [76] that have been implicated in the pathophysiology of depression. Chronic stress, which is a risk factor for MDD, has been proposed to lead to increased inflammation [14], which in turn disrupts neural circuits involved in interoceptive processing [15]. Additionally, cytokines can affect the function of neurons and glia in the brain, leading to altered neural activity and connectivity [77]. Therefore, the association between lower miR-93 expression and higher serum concentrations of IL-1ra, IL-6, TNF, and leptin in individuals with MDD, might be interpreted to suggest that a low miR-93 expression level fails to regulate inflammatory cytokines in MDD. Again, further studies are needed to validate and extend this notion.

Strengths

We focused on evaluating how a neuronal process could be associated with interoceptive signaling using the innovative technique of NEEV isolation. For this, NEEV were isolated with the use of the transmembrane L1 cell adhesion molecule (L1CAM/

CD171). A recent review article reported concern about using L1CAM/CD171 enriched EVs [78], due to the expression of L1CAM in other tissues of the body. We took careful steps to characterize and verify NEEVs following the MISEV2018 guidelines [56], including: (1) flow cytometry of CD63 and CD171; (2) western blot analysis of EV surface markers, CD171 and CD81, EV internal marker – Alix, the EV negative marker – calnexin, and the contaminant marker – APOA1; (3) EV and NEEV particle size and concentration measurements using the MRPS technology; (4) transmission electron microscopy imaging of EV and NEEV; (5) EV-depleted samples used as negative controls; and (6) the use of thrombin treatment for removal of fibrinogen from plasma, which potentially affects plasma EV separation and characterization. Also, data confirmed that the neuronal cell-specific marker, miR-9, was expressed at a much higher level in NEEV than EV, supporting the enriched neuronal origin of NEEV [55]. Lastly, several labs continue to pursue candidates for neuronal-specific markers for enrichment, such as NCAM and ATP1A3 [79, 80]. To this end, we further confirmed the neuronal origin of our NEEVs by identifying positive immunoreactivity of NCAM and ATP1A3 with western blot analysis.

Limitations

While this study revealed new insight into the possible role of NEEV miR-93 in interoception, there are several limitations. First, more than half of MDD patients were taking SSRIs, raising the possibility of serotonergic influences on the results. We believe this is unlikely as there was no difference on the VIA task or NEEV miR-93 expression between unmedicated MDD and SSRI-medicated individuals. Future work may address this by repeating the study in unmedicated participants only. Second, other unmeasured factors could have potentially affected our results, such as other types of medication, genetics, diet, and socio-economic status. Third, although we characterized the neuronal enrichment of NEEV, we were unable to further subdivide the NEEV populations to determine neuron type. Future studies should be undertaken to replicate these findings, refine the observed relationships to specific neuronal subtypes, and longitudinally evaluate the degree to which NEEV signaling fluctuates with interoceptive and affective changes, reflecting the varied emotional landscape of depression.

CONCLUSIONS

This study suggests that MDD is associated with lower NEEV miR-93 expression, which may lead to interoceptive processing dysfunctions through altered epigenetic modulation of insular function, whereas healthy individuals may be more reactive to stress-induced regulation of miR-93 expression during interoceptive processing. The combination of neuroimaging and brain-enriched extracellular vesicle approaches provides an exciting opportunity to discover novel cellular disease targets for depression.

DATA AVAILABILITY

The data that support the findings of this study are available from corresponding author upon reasonable request.

REFERENCES

- Khalsa SS, Adolphs R, Cameron OG, Critchley HD, Davenport PW, Feinstein JS, et al. Interoception and mental health: a roadmap. *Biol Psychiatry Cogn Neurosci Neuroimaging*. 2018;3:501–13.
- Barrett LF, Quigley KS, Hamilton P. An active inference theory of allostasis and interoception in depression. *Philos Trans R Soc Lond B Biol Sci*. 2016;371:20160011.
- Khalsa SS, Lapidus RC. Can interoception improve the pragmatic search for biomarkers in psychiatry? *Front Psychiatry*. 2016;7:121.
- Paulus MP, Stein MB. Interoception in anxiety and depression. *Brain Struct Funct*. 2010;214:451–63.
- Avery JA, Drevets WC, Moseman SE, Bodurka J, Barcalow JC, Simmons WK. Major depressive disorder is associated with abnormal interoceptive activity and functional connectivity in the insula. *Biol Psychiatry*. 2014;76:258–66.
- Craig AD. Interoception: the sense of the physiological condition of the body. *Curr Opin Neurobiol*. 2003;13:500–5.
- Paulus MP, Stein MB. An insular view of anxiety. *Biol Psychiatry*. 2006;60:383–7.
- Seth AK, Critchley HD. Extending predictive processing to the body: emotion as interoceptive inference. *Behav Brain Sci*. 2013;36:227–8.
- Seth AK, Friston KJ. Active interoceptive inference and the emotional brain. *Philos Trans R Soc Lond B Biol Sci*. 2016;371:20160007.
- Nord CL, Lawson RP, Dalgleish T. Disrupted dorsal mid-insula activation during interoception across psychiatric disorders. *Am J Psychiatry*. 2021;178:761–70.
- Hsueh B, Chen R, Jo Y, Tang D, Raffiee M, Kim YS, et al. Cardiogenic control of affective behavioural state. *Nature*. 2023;15:292–9.
- Barrett LF, Simmons WK. Interoceptive predictions in the brain. *Nat Rev Neurosci*. 2015;16:419–29.
- Simmons WK, Burrows K, Avery JA, Kerr KL, Taylor A, Bodurka J, et al. Appetite changes reveal depression subgroups with distinct endocrine, metabolic, and immune states. *Mol Psychiatry*. 2020;25:1457–68.
- Beurel E, Toups M, Nemeroff CB. The bidirectional relationship of depression and inflammation: double trouble. *Neuron*. 2020;107:234–56.
- Savitz J, Harrison NA. Interoception and inflammation in psychiatric disorders. *Biol Psychiatry Cogn Neurosci Neuroimaging*. 2018;3:514–24.
- Milaneschi Y, Simmons WK, van Rossum EFC, Penninx BW. Depression and obesity: evidence of shared biological mechanisms. *Mol Psychiatry*. 2019;24:18–33.
- O'Rahilly S. 20 years of leptin: what we know and what the future holds. *J Endocrinol*. 2014;223:E1–3.
- La Cava A. Leptin in inflammation and autoimmunity. *Cytokine*. 2017;98:51–58.
- Kalluri R, LeBleu VS. The biology, function, and biomedical applications of exosomes. *Science*. 2020;367:eaau6977.
- Fineberg SK, Kosik KS, Davidson BL. MicroRNAs potentiate neural development. *Neuron*. 2009;64:303–9.
- Nowak JS, Michlewski G. miRNAs in development and pathogenesis of the nervous system. *Biochem Soc Trans*. 2013;41:815–20.
- Saeedi S, Israel S, Nagy C, Turecki G. The emerging role of exosomes in mental disorders. *Transl Psychiatry*. 2019;9:122.
- Ventura A, Young AG, Winslow MM, Lintault L, Meissner A, Erkland SJ, et al. Targeted deletion reveals essential and overlapping functions of the miR-17 through 92 family of miRNA clusters. *Cell*. 2008;132:875–86.
- Lattanzi A, Gentner B, Como D, Di Tomaso T, Mestdagh P, Speleman F, et al. Dynamic activity of miR-125b and miR-93 during murine neural stem cell differentiation in vitro and in the subventricular zone neurogenic niche. *PLoS ONE*. 2013;8:e67411.
- Chen X, Yang H, Zhou X, Zhang L, Lu X. MiR-93 Targeting EphA4 promotes neurite outgrowth from spinal cord neurons. *J Mol Neurosci*. 2016;58:517–24.
- Brett JO, Renault VM, Rafalski VA, Webb AE, Brunet A. The microRNA cluster miR-106b~25 regulates adult neural stem/progenitor cell proliferation and neuronal differentiation. *Aging*. 2011;3:108–24.
- Wang Y, Chen S, Wang J, Liu Y, Chen Y, Wen T, et al. MicroRNA-93/STAT3 signalling pathway mediates retinal microglial activation and protects retinal ganglion cells in an acute ocular hypertension model. *Cell Death Dis*. 2021;12:41.
- Yan XT, Ji LJ, Wang Z, Wu X, Wang Q, Sun S, et al. MicroRNA-93 alleviates neuropathic pain through targeting signal transducer and activator of transcription 3. *Int Immunopharmacol*. 2017;46:156–62.
- Figuroa-Hall LK, Paulus MP, Savitz J. Toll-Like receptor signaling in depression. *Psychoneuroendocrinology*. 2020;121:104843.
- Gao H, Xiao D, Gao L, Li X. MicroRNA-93 contributes to the suppression of lung inflammatory responses in LPS-induced acute lung injury in mice via the TLR4/MyD88/NF-κB signaling pathway. *Int J Mol Med*. 2020;46:561–70.
- Wang L, Yang JW, Lin LT, Huang J, Wang XR, Su XT, et al. Acupuncture attenuates inflammation in microglia of vascular dementia rats by inhibiting miR-93-mediated TLR4/MyD88/NF-κB signaling pathway. *Oxid Med Cell Longev*. 2020;2020:8253904.
- He Z, Wang H, Yue L. Endothelial progenitor cells-secreted extracellular vesicles containing microRNA-93-5p confer protection against sepsis-induced acute kidney injury via the KDM6B/H3K27me3/TNF-alpha axis. *Exp Cell Res*. 2020;395:112173.
- Milluzzo A, Maugeri A, Barchitta M, Sciacca L, Agodi A. Epigenetic mechanisms in Type 2 diabetes retinopathy: a systematic review. *Int J Mol Sci*. 2021;22:10502.
- Fernandes BS, Salagre E, Enduru N, Grande I, Vieta E, Zhao Z. Insulin resistance in depression: a large meta-analysis of metabolic parameters and variation. *Neurosci Biobehav Rev*. 2022;139:104758.
- Shelton RC, Miller AH. Inflammation in depression: is adiposity a cause? *Dialogues Clin Neurosci*. 2011;13:41–53.

36. Cioffi M, Vallespinos-Serrano M, Trabulo SM, Fernandez-Marcos PJ, Firment AN, Vazquez BN, et al. miR-93 controls adiposity via inhibition of sirt7 and Tbx3. *Cell Rep*. 2015;12:1594–605.
37. Penninx B, Lange SMM. Metabolic syndrome in psychiatric patients: overview, mechanisms, and implications. *Dialogues Clin Neurosci*. 2018;20:63–73.
38. Badal SS, Wang Y, Long J, Corcoran DL, Chang BH, Truong LD, et al. miR-93 regulates Msk2-mediated chromatin remodelling in diabetic nephropathy. *Nat Commun*. 2016;7:12076.
39. Golden SA, Christoffel DJ, Heshmati M, Hodes GE, Magida J, Davis K, et al. Epigenetic regulation of RAC1 induces synaptic remodeling in stress disorders and depression. *Nat Med*. 2013;19:337–44.
40. Victor TA, Khalsa SS, Simmons WK, Feinstein JS, Savitz J, Aupperle RL, et al. Tulsa 1000: a naturalistic study protocol for multilevel assessment and outcome prediction in a large psychiatric sample. *BMJ Open*. 2018;8:e016620.
41. Sheehan DV, Lecrubier Y, Sheehan KH, Amorim P, Janavs J, Weiller E, et al. The Mini-International Neuropsychiatric Interview (M.I.N.I.): the development and validation of a structured diagnostic psychiatric interview for DSM-IV and ICD-10. *J Clin Psychiatry*. 1998;59:34–57.
42. Kroenke K, Spitzer RL, Williams JB. The PHQ-9: validity of a brief depression severity measure. *J Gen Intern Med*. 2001;16:606–13.
43. Burrows K, DeVille DC, Cosgrove KT, Kuplicki RT, Paulus MP, Aupperle R, et al. Impact of serotonergic medication on interoception in major depressive disorder. *Biol Psychol*. 2022, 169:108286.
44. Cella D, Riley W, Stone A, Rothrock N, Reeve B, Yount S, et al. The Patient-Reported Outcomes Measurement Information System (PROMIS) developed and tested its first wave of adult self-reported health outcome item banks: 2005–2008. *J Clin Epidemiol*. 2010;63:1179–94.
45. Burrows K, Figueroa-Hall LK, Kuplicki R, Stewart JL, Alarbi AM, Ramesh R, et al. Neuronally-enriched exosomal microRNA-27b mediates acute effects of ibuprofen on reward-related brain activity in healthy adults: a randomized, placebo-controlled, double-blind trial. *Sci Rep*. 2022;12:861.
46. Mustapic M, Eitan E, Werner JK Jr., Berkowitz ST, Lazaropoulos MP, Tran J, et al. plasma extracellular vesicles enriched for neuronal origin: a potential window into brain pathologic processes. *Front Neurosci*. 2017;11:278.
47. Winston CN, Romero HK, Ellisman M, Naus S, Julovich DA, Conger T, et al. Assessing neuronal and astrocyte derived exosomes from individuals with mild traumatic brain injury for markers of neurodegeneration and cytotoxic activity. *Front Neurosci*. 2019;13:1005.
48. Pulliam L, Sun B, Mustapic M, Chawla S, Kapogiannis D. Plasma neuronal exosomes serve as biomarkers of cognitive impairment in HIV infection and Alzheimer's disease. *J Neurovirol*. 2019;25:702–9.
49. Avery JA, Burrows K, Kerr KL, Bodurka J, Khalsa SS, Paulus MP, et al. How the brain wants what the body needs: the neural basis of positive alliesthesia. *Neuropsychopharmacology*. 2017;42:822–30.
50. DeVille DC, Kuplicki R, Stewart JL, Tulsa I, Paulus MP, Khalsa SS. Diminished responses to bodily threat and blunted interoception in suicide attempters. *eLife*. 2020;9:e51593.
51. Kerr KL, Moseman SE, Avery JA, Bodurka J, Zucker NL, Simmons WK. Altered Insula Activity during Visceral Interoception in Weight-Restored Patients with Anorexia Nervosa. *Neuropsychopharmacology*. 2016;41:521–8.
52. Simmons WK, Avery JA, Barcalow JC, Bodurka J, Drevets WC, Bellgowan P. Keeping the body in mind: insula functional organization and functional connectivity integrate interoceptive, exteroceptive, and emotional awareness. *Hum Brain Mapp*. 2013;34:2944–58.
53. Stewart JL, Khalsa SS, Kuplicki R, Puhl M, Investigators T, Paulus MP. Interoceptive attention in opioid and stimulant use disorder. *Addict Biol*. 2020;25:e12831.
54. Cox RW. AFNI: software for analysis and visualization of functional magnetic resonance neuroimages. *Comput Biomed Res*. 1996;29:162–73.
55. Cha DJ, Mengel D, Mustapic M, Liu W, Selkoe DJ, Kapogiannis D, et al. miR-212 and miR-132 Are downregulated in neurally derived plasma exosomes of Alzheimer's patients. *Front Neurosci*. 2019;13:1208.
56. Thery C, Witwer KW, Aikawa E, Alcaraz MJ, Anderson JD, Andriantsitohaina R, et al. Minimal information for studies of extracellular vesicles 2018 (MISEV2018): a position statement of the International Society for Extracellular Vesicles and update of the MISEV2014 guidelines. *J Extracell Vesicles*. 2018;7:1535750.
57. Ding L, Ni J, Yang F, Huang L, Deng H, Wu Y, et al. Promising therapeutic role of miR-27b in tumor. *Tumour Biol*. 2017;39:1010428317691657.
58. Golan M, Schreiber G, Avissar S. Antidepressant-induced differential ubiquitination of β -arrestins 1 and 2 in mononuclear leucocytes of patients with depression. *Int J Neuropsychopharmacol*. 2013;16:1745–54.
59. Li Q, Korte M, Sajikumar S. Ubiquitin-proteasome system inhibition promotes long-term depression and synaptic tagging/capture. *Cereb Cortex*. 2016;26:2541–8.
60. Mouri A, Ikeda M, Koseki T, Iwata N, Nabeshima T. The ubiquitination of serotonin transporter in lymphoblasts derived from fluvoxamine-resistant depression patients. *Neurosci Lett*. 2016;617:22–26.
61. Dillon DG, Pizzagalli DA. Mechanisms of memory disruption in depression. *Trends Neurosci*. 2018;41:137–49.
62. Schweizer S, Kievit RA, Emery T, Henson RN. Symptoms of depression in a large healthy population cohort are related to subjective memory complaints and memory performance in negative contexts. *Psychol Med*. 2018;48:104–14.
63. Kabir ZD, Martinez-Rivera A, Rajadhyaksha AM. From gene to behavior: L-type calcium channel mechanisms underlying neuropsychiatric symptoms. *Neurotherapeutics*. 2017;14:588–613.
64. Nakao A, Matsunaga Y, Hayashida K, Takahashi N. Role of oxidative stress and Ca(2+) signaling in psychiatric disorders. *Front Cell Dev Biol*. 2021;9:615569.
65. Pariante CM. Increased inflammation in depression: a little in all, or a lot in a few? *Am J Psychiatry*. 2021;178:1077–9.
66. Dantzer R, O'Connor JC, Freund GG, Johnson RW, Kelley KW. From inflammation to sickness and depression: when the immune system subjugates the brain. *Nat Rev Neurosci*. 2008;9:46–56.
67. Dowlati Y, Herrmann N, Swardfager W, Liu H, Sham L, Reim EK, et al. A meta-analysis of cytokines in major depression. *Biol Psychiatry*. 2010;67:446–57.
68. Tian F, Yuan C, Hu L, Shan S. MicroRNA-93 inhibits inflammatory responses and cell apoptosis after cerebral ischemia reperfusion by targeting interleukin-1 receptor-associated kinase 4. *Exp Ther Med*. 2017;14:2903–10.
69. Xu Y, Jin H, Yang X, Wang L, Su L, Liu K, et al. MicroRNA-93 inhibits inflammatory cytokine production in LPS-stimulated murine macrophages by targeting IRAK4. *FEBS Lett*. 2014;588:1692–8.
70. Milaneschi Y, Lamers F, Bot M, Drent ML, Penninx BW. Leptin dysregulation is specifically associated with major depression with atypical features: evidence for a mechanism connecting obesity and depression. *Biol Psychiatry*. 2017;81:807–14.
71. Lamers F, Vogelzangs N, Merikangas KR, de Jonge P, Beekman AT, Penninx BW. Evidence for a differential role of HPA-axis function, inflammation and metabolic syndrome in melancholic versus atypical depression. *Mol Psychiatry*. 2013;18:692–9.
72. Critchley HD, Wiens S, Rotshtein P, Ohman A, Dolan RJ. Neural systems supporting interoceptive awareness. *Nat Neurosci*. 2004;7:189–95.
73. Craig AD. How do you feel—now? The anterior insula and human awareness. *Nat Rev Neurosci*. 2009;10:59–70.
74. Klabunde M, Weems CF, Raman M, Carrion VG. The moderating effects of sex on insula subdivision structure in youth with posttraumatic stress symptoms. *Depress Anxiety*. 2017;34:51–58.
75. Critchley Hugo D, Harrison Neil A. Visceral Influences on Brain and Behavior. *Neuron*. 2013;77:624–38.
76. Raison CL, Miller AH. Pathogen–host defense in the evolution of depression: insights into epidemiology, genetics, bioregional differences and female preponderance. *Neuropsychopharmacology*. 2017;42:5–27.
77. Ferro A, Auguste YSS, Cheadle L. Microglia, cytokines, and neural activity: unexpected interactions in brain development and function. *Front Immunol*. 2021;12:703527.
78. Gomes DE, Witwer KW. L1CAM-associated extracellular vesicles: a systematic review of nomenclature, sources, separation, and characterization. *J Extracell Biol*. 2022;1:e35.
79. Fiandaca MS, Kapogiannis D, Mapstone M, Boxer A, Eitan E, Schwartz JB, et al. Identification of preclinical Alzheimer's disease by a profile of pathogenic proteins in neurally derived blood exosomes: a case-control study. *Alzheimers Dement*. 2015;11:600–607.e601.
80. You Y, Zhang Z, Sultana N, Ericsson M, Martens YA, Sun M, et al. ATP1A3 as a target for isolating neuron-specific extracellular vesicles from human brain and biofluids. *Sci Adv*. 2023;9:eadi3647.

ACKNOWLEDGEMENTS

The blood processing and EV isolation were conducted at the Integrative Immunology Center (IIC), School of Community Medicine, The University of Oklahoma, Tulsa, OK. The authors wish to thank the IIC staff Ashlee Rempel and Brenda Davis for their work and support involved in the data collection.

AUTHOR CONTRIBUTIONS

KB contributed to research design, data collection, data analysis, and manuscript writing, and review; LKF contributed to data analysis, manuscript writing and preparation; JLS contributed to manuscript writing and preparation; AMA contributed to EV western blot analysis, manuscript writing and preparation; RK contributed to imaging data collection and analysis, manuscript writing and preparation; BNH contributed to EV isolation protocols, western blot troubleshooting, and reviewing of the manuscript; CT contributed to EV flow cytometry data collection and analysis; VBR contributed to EV study design, and reviewing of the manuscript; BAM contributed to supervision of miRNA data analysis, and reviewing of the manuscript; RR contributed

to EV nanoparticle analysis, review and editing of the manuscript; JBS contributed to critical manuscript review; TAV contributed to T1000 study design, review and editing of the manuscript; RA contributed to review and editing of the manuscript; JBS contributed to critical manuscript review; TKT contributed to study design, EV western blot and flow cytometry analysis, critical manuscript writing and review; SSK contributed to critical manuscript writing and review; MPP contributed to study design, supervision of data collection and analysis, manuscript writing and preparation, and critical review of the manuscript. All authors reviewed the manuscript.

FUNDING

This work was supported by the National Institute of General Medical Sciences Center Grant Award (P20GM121312 to MPP), National Institute on Drug Abuse (R01DA050677 to JLS); National Institute of Mental Health (K99MH126950 to LFH and R01MH127225 to SSK); and The William K. Warren Foundation.

COMPETING INTERESTS

The authors declare no competing interests.

ADDITIONAL INFORMATION

Supplementary information The online version contains supplementary material available at <https://doi.org/10.1038/s41398-024-02907-x>.

Correspondence and requests for materials should be addressed to Kaiping Burrows.

Reprints and permission information is available at <http://www.nature.com/reprints>

Publisher's note Springer Nature remains neutral with regard to jurisdictional claims in published maps and institutional affiliations.



Open Access This article is licensed under a Creative Commons Attribution 4.0 International License, which permits use, sharing, adaptation, distribution and reproduction in any medium or format, as long as you give appropriate credit to the original author(s) and the source, provide a link to the Creative Commons licence, and indicate if changes were made. The images or other third party material in this article are included in the article's Creative Commons licence, unless indicated otherwise in a credit line to the material. If material is not included in the article's Creative Commons licence and your intended use is not permitted by statutory regulation or exceeds the permitted use, you will need to obtain permission directly from the copyright holder. To view a copy of this licence, visit <http://creativecommons.org/licenses/by/4.0/>.

© The Author(s) 2024